Substrate effects on surface-plasmon spectra in metal-island films

P. Royer, J. P. Goudonnet, R. J. Warmack, and T. L. Ferrell
Health and Safety Research Division, Oak Ridge National Laboratory, Oak Ridge, Tennessee 37831
(Received 23 September 1986)

The effects of the local dielectric environment on the surface-plasmon resonances of annealed metal-island films are studied experimentally and modeled theoretically. Silver-island films were annealed to produce spheroidal shaped particles which exhibit well-resolved resonances in polarized, angle-resolved, absorption spectra. These resonances are shifted in different amounts by the depolarizing interaction with the underlying substrate. They are also affected by additional dielectric coverages or separation of the particle film from the substrate. Cross-section calculations based upon a nonretarded, single-particle, dielectric interaction for these various configurations are presented and found to be in agreement with experimental observations.

I. INTRODUCTION

Metal-island films have long been studied as physically interesting and readily prepared samples evincing nanometer-scale thickness, surface melting, variation in the peak wavelength of optical absorbance, and electrically discontinuous behavior.[1] At temperatures well below the melting point, surface-melting migration causes gold and silver films of 0.5 to 5 nm thickness to form a stochastic array of particulates resembling oblate spheroids with all minor axes oriented normal to the substrate (typically glass, quartz, or silicon). The literature on metal-island films is worthy of a review paper, and we shall not attempt a complete bibliography here. The present study is a natural progression of our previous papers on optical studies and investigations of radiative decay of surface plasmons stimulated by electron bombardment.[2–5] In this work we present an attempt at correlating the surface-plasmon spectrum of heat-treated silver-island films with the optical properties of the substrate upon which they reside. Section II describes the experimental techniques employed in our studies, and Sec. III presents an elementary model of the substrate's effects on the surface-plasmon spectrum. In Sec. IV we give a comparison of the theory and data, while in Sec. V we give our conclusions.

Since the substrate upon which the silver film is deposited may influence the shape of the particulates formed as a result of varying surface mobility, each substrate utilized in our study is first coated with evaporated quartz of a given thickness. Thus, all films are deposited and heat treated on evaporated quartz to produce nearly identical films. The substrate underlying the quartz is varied, and the experiments are repeated for several different values of the quartz thickness. Figure 1 shows a 4-nm silver film on silicon which has a natural oxide layer. All other variables being the same, these films are basically the same as films deposited on evaporated quartz, a convenience for obtaining electron micrographs. The films are electrically discontinuous and display two peaks in their optical absorbance for *p*-polarized incident light. Figures 2 and 3 show the same film following heat treatment.

As Fig. 3 shows, the particles resemble isolated oblate

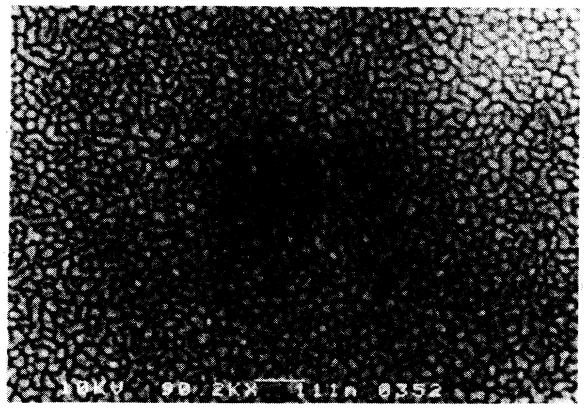

FIG. 1. Scanning electron micrograph of a thin (5-nm) silver evaporation on silicon at room temperature. Bar indicates a length of 111 nm.

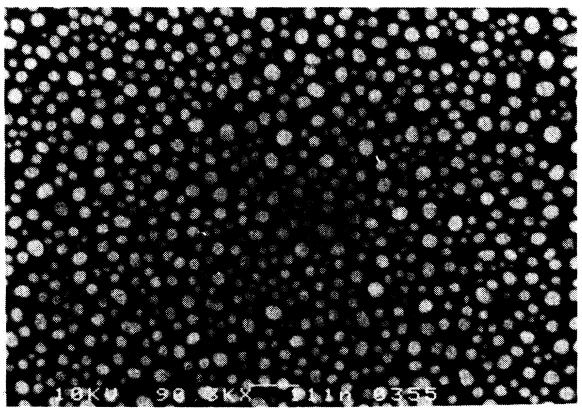

FIG. 2. Evaporated silver film on silicon after a 1-min anneal at 200 °C. Same scale as Fig. 1.

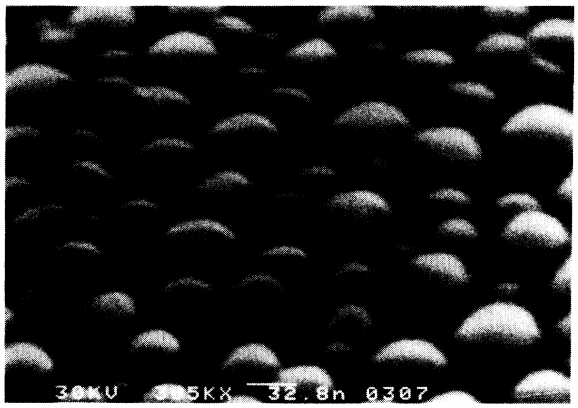

FIG. 3. Evaporated and annealed silver film on silicon viewed at 60° from normal showing the oblate shape of the particles. Bar indicates a length of 32.8 nm.

spheroids of sufficiently small size (major axis is ~30—40 nm) that one may neglect retardation effects in analyzing their optical properties. We previously have shown a single-particle model to be useful in describing the surface-plasmon resonances, as cited above.[4] Various heat treatments red shift the optically induced, lower-energy, surface plasmon by various amounts, a phenomenon we ascribe to the different shapes produced. The higher-energy peak in the optical absorbance is less shifted due to the steep slope of the real part of the dielectric function of silver $\epsilon_1(\omega)$ in that frequency range. Also, equally important is the fact that the peak is pinned between $\epsilon_1=0$ and the spherical resonance. Since the imaginary part of the dielectric function $\epsilon_2(\omega)$ grows with decreasing frequency in the visible region, the longer-wavelength resonance broadens correspondingly and is attributed to the surface-plasmon mode which is stimulated by the component of the incident electric field along the major axis. The surface-plasmon peak at longer wavelength is governed by a relatively wide range of ϵ_1 at resonance and is much more sensitive to the particulate shape. The short-wavelength mode is stimulated normal to the surface along the minor axis. By correlating the position and width of the two surface-plasmon modes with theory, one hopes to optically determine the shape (minor—to—major-axis ratio) of particulates much smaller than the wavelength of light. This is clearly impossible using elastic scattering data and is a particularly interesting possibility using inelastic scattering. We note that the elastic scattering cross section diminishes with decreasing volume as the square of the volume, whereas the absorption diminishes only in proportion to the volume. For our films the elastic scattering is a few percent of the total. The possibility of shape determination is thus more feasible, although it is limited by how carefully the substrate effect and interparticle interactions can be separated from other contributions to the position and width of the surface-plasmon resonances. One problem with making such a delineation is that there is a variation in shape of the particulates which broadens the absorbance peaks. Fortunately, the samples appear to display a reasonably narrow distribution of shapes as partially confirmed by shadow-casting techniques. Detailed measurements of greater accuracy may be forthcoming with the advent of scanning-tunneling electron microscopy.[6] At present we are largely restricted to an iterative approach of comparing improving theory with improving experiments on surface-plasmon excitation.

Although metal-island films have been used in studies of surface-enhanced Raman scattering (SERS), they do not serve as the optimum sample for this purpose.[7] Samples that are more difficult to produce are many times more effective in SERS.[8] However, silver-island films show two polarization-dependent surface-plasmon resonances in the visible to uV region, and the higher-energy mode can be eliminated from stimulation by using only *s*-polarized light. Thus, it is possible in principle to delineate the surface-plasmon contribution to SERS and other phenomena by using the low-wavelength mode. The basic reasons that the peak SERS enhancement has not yet been studied in this fashion are the relatively small enhancements by metal-island films and the fact that the high-energy mode is accompanied by considerable fluorescence noise from the metal. On the other hand, samples which give better enhancements have not been so well characterized optically and have rather broad resonances relative to the metal-island films. By judicious choice of the substrate on which microstructures are formed and of the microstructure geometry, it may be possible to overcome such problems. The substrate causes a red shift of the surface-plasmon energy, though not as large a shift as when the microstructures are completely surrounded by a dielectric. Sufficient red shift permits removal of the resonances from the spectral region in which fluorescence is a problem. Of course, the damping in silver broadens the surface-plasmon peaks at the longer wavelengths in the visible region, and hence one sacrifices signal to some extent. However, the sacrifice is not prohibitively large for samples of a narrow range of shapes, and the major problem is more one of keeping the two surface-plasmon peaks separated. Similar problems occur with the retardation red shift when larger microstructures are used. It is clear that a detailed understanding of the position and width of the surface-plasmon peaks as a function of the microstructure parameters and the type of substrate is highly desirable for understanding SERS and for developing a method of shape determination optically.

Among the factors influencing the surface-plasmon spectrum of metal-island films is the degree of interaction of the particles. This factor is difficult to calculate from first principles and is difficult to measure directly. Approximation methods must be employed, but the order of the approximation which may be necessary would require that tedious calculations be carried out. Before employing an extensive calculation, it is prudent to test simple models. It might well prove that explicit calculation of the interparticle coupling is of minimal value without experimental tests in which the interparticle spacing can be systematically varied and in which the substrate influence is isolated. Until such data are available, we offer the simple alternative discussed in Sec. III. Eventually, the delineation of interaction effects will be of great help in

understanding coupling between small particles, and we hope to undertake relevant experiments in the near future. The extensive use of small-particle catalysts in the chemical industry is only one of the areas that could benefit from such detailed knowledge. Again, the silver-island films, while not the most valuable for direct use, do much in helping to understand other important samples.

II. EXPERIMENTAL DETAILS

Two substrates with a high index of refraction relative to silica were chosen for study of the effect of the substrate upon the surface-plasmon resonances of illuminated silver particles. Lead fluoride substrates were made by direct evaporation onto fused silica slides by an electron beam, cryopumped evaporator. Titanium oxide films were made by evaporation of titanium followed by oxidation at 550 °C in a water vapor atmosphere for 10 min. The films in both cases were approximately 100 nm or greater, which is thick enough to fully relax the electric fields from the surface-plasmon excitation. Thin films of high-purity silica were subsequently evaporated at 0.1 nm/s at a pressure less than 1×10^{-4} Pa. The silver films were formed by one evaporation of 4-nm high-purity silver followed by heat treatment at 200 °C for 1 min. Higher temperatures were found to give more variation from sample to sample in the particulate shape. The optical absorption of these films was measured by transmission in a dual-beam spectrophotometer equipped with rotational stages for angular measurements and polarizers which could be oriented either parallel (p polarized) or perpendicular (s polarized) to the plane of incidence. The wavelength of the resonance for the tangential dipole mode was determined from the peak in the absorption spectrum taken at normal incidence. The reference beam contained a slide identical to the sample but without a silver film.

We also took spectra on several samples which were surrounded with xylene as an index-matching fluid and covered with a silica slide. In this case the silver particles appear to be totally immersed in an approximately uniform dielectric. Incidence angles of the light striking the particles were limited to less than about 40° for this configuration due to the refraction in the fluid.

III. THEORY

The polarizability of an oblate spheroidal particulate of silver at angular frequency ω has components $\alpha_R(\omega)$ and $\alpha_z(\omega)$ along the major axes and minor axis, respectively. Each polarizability component has a resonance at a frequency for which the real part $\epsilon_1(\omega)$ of the dielectric function of silver is a particular value. For $\alpha_R(\omega)$ this value is here labeled ϵ_{11}, while for $\alpha_z(\omega)$ the value is labeled ϵ_{10}. The subscripts are mode labels, with the first subscript indicating a dipole mode and the second subscript being the azimuthal index, zero for azimuthal symmetry and unity for the only azimuthal mode. One finds from simple electrodynamics[4]

$$\alpha_R(\omega)=\frac{V}{2\pi Q}\frac{\epsilon(\omega)-1}{\epsilon(\omega)-\epsilon_{11}}\ , \tag{1}$$

and

$$\alpha_z(\omega)=\frac{V}{4\pi(1-Q)}\frac{\epsilon(\omega)-1}{\epsilon(\omega)-\epsilon_{11}}\ , \tag{2}$$

where the volume of the spheroid is V and

$$Q=\eta_0(1+\eta_0^2)(\cot^{-1}\eta_0)-\eta_0\ . \tag{3}$$

The oblate spheroidal coordinate η_0 is related to the ratio R_0 of the minor to the major axis by

$$R_0=\frac{\eta_0}{(1+\eta_0^2)^{1/2}} \tag{4}$$

for $0\le\eta_0\le\infty$. Also,

$$\epsilon_{11}=1-\frac{2}{Q}\ , \tag{5}$$

$$\epsilon_{10}=1-\frac{1}{1-Q}\ , \tag{6}$$

which are each negative real numbers. The absorbance of an array of oblate spheroids depends upon the imaginary part of the polarizabilities. Before considering this, however, we wish to consider a model for the influence of the substrates on which the particulates reside. The model is based upon consideration of how a thin film is influenced by a substrate. In an ordinary continuous thin film, there are two surface-plasmon modes, a symmetric or tangential mode and an antisymmetric or normal mode. These correspond to the roots of a quadratic dispersion relation obtained from simple electrodynamics. Using a nonretarded formalism, one obtains the dispersion relation by solving for the scalar electric potential and satisfying the boundary conditions.[9] For a thin film of thickness b bounded by vacuum, the surface plasmon of wave vector K and angular frequency ω is described by the resulting quadratic dispersion relation:

$$\epsilon^2(\omega)+2\epsilon(\omega)\coth(Kb)+1=0 \tag{7}$$

or

$$\epsilon^2(\omega)-\epsilon(\omega)(\epsilon_A+\epsilon_S)+\epsilon_A\epsilon_S=0\ , \tag{8}$$

where the root of the antisymmetric mode is

$$\epsilon_A=-\tanh\left[\frac{Kb}{2}\right] \tag{9}$$

and the root for the symmetric mode is

$$\epsilon_S=-\coth\left[\frac{Kb}{2}\right]\ . \tag{10}$$

These roots are the thin-film analogues of ϵ_{10} and ϵ_{11}, respectively. For instance, ϵ_{10} corresponds to charge oscillations on an oblate spheroid with opposite signs on either side of the particle along the direction of the minor axis, which is the analogue of the foil thickness.

If the thin foil resides on a semi-infinite, plane-bounded substrate of dielectric function $\epsilon^0(\omega)$, then Eq. (8) becomes

$$\epsilon^2(\omega)-\epsilon(\omega)\left[\frac{\epsilon^0(\omega)+1}{2}\right](\epsilon_A+\epsilon_S)+\epsilon_0\epsilon_A\epsilon_S=0\ . \tag{11}$$

When a 4-nm film of silver is deposited on a substrate and heat treated at 200 °C for 1 min, the film appears in electron micrographs as a collection of isolated particulates resembling oblate spheroids. Unlike a continuous thin film, surface-plasmon excitation by photons incident in vacuum occurs directly. The total cross section including inelastic scattering is found for p-polarized light to be[4]

$$\sigma=\frac{4\pi\omega}{c}\,\mathrm{Im}(\alpha_R\cos^2\theta+\alpha_z\sin^2\theta)\ , \tag{12}$$

where θ is the angle of incidence. Since the particulates reside close together relative to a wavelength of light at the surface-plasmon energy and since the dielectric function $\epsilon^0(\omega)$ may affect the surface-plasmon spectrum, Eq. (12) is only approximate. However, the approximation can be improved by modifying the polarizabilities to take account of these effects. A simple model can be obtained by writing a quadratic equation for ϵ_{11} and ϵ_{10}; viz.,

$$\epsilon^2(\omega)-\epsilon(\omega)(\epsilon_{11}+\epsilon_{10})+\epsilon_{11}\epsilon_{10}=0\ , \tag{13}$$

and then modifying the equation in the same manner that Eq. (8) is modified to produce Eq. (11). One thus obtains

$$\epsilon^2(\omega)-\epsilon(\omega)(\epsilon_{11}+\epsilon_{10})\left[\frac{\epsilon^0(\omega)+1}{2}\right]+\epsilon_0(\omega)\epsilon_{11}\epsilon_{10}=0\ . \tag{14}$$

The particulates are small compared to a wavelength and spaced much less than a wavelength apart. Also, electron micrographs show the particulates to differ considerably from sphericity. The modification of the vacuum equation is thus assumed to be identical to the modification of the vacuum-bounded thin-film eigenequation. The polarizabilities are then modified by replacing ϵ_{11} and ϵ_{10} by the roots of Eq. (14).

In order to test the usefulness of this modified thin-film approximation (MTFA), we have compared shape determinations from absorbance measurements of silver films on quartz with the shapes of the particulates measured by shadow casting and analysis of electron micrographs. Encouraged by the results, which are unfortunately limited by the inherent errors in shadow casting, we embarked upon a more systematic test. We have employed a number of substrates other than quartz, but the shape of the particulates is influenced by the type of substrate. To overcome this, we evaporated selected thicknesses of quartz onto each substrate. This had the additional advantage of offering measurements of the dependence of the results upon distance from the substrate. The MTFA for such experiments is detailed below.

Consider a plane-bounded semi-infinite substrate of dielectric function $\bar{\epsilon}(\omega)$. Let this be overcoated with a quartz layer of dielectric function $\epsilon^0(\omega)$ and thickness a_1. Consider a thin film of a metal with dielectric function $\epsilon(\omega)$ and thickness a deposited on the quartz. The dispersion relation for surface plasmons is then easily calculated to be

$$\epsilon^2(\omega)+\epsilon(\omega)[(1+f\epsilon^0(\omega)]\coth(Ka)+f\epsilon^0(\omega)=0\ , \tag{15}$$

where

$$f=\frac{\epsilon^0(\omega)+\bar{\epsilon}(\omega)\coth(Ka_1)}{\epsilon^0(\omega)\coth(Ka_1)+\bar{\epsilon}(\omega)}\ . \tag{16}$$

If $\bar{\epsilon}(\omega)=\epsilon^0(\omega)$, this is the same as Eq. (11). Just as in modifying Eq. (13) to produce Eq. (14), we assume Eq. (15) to here be modified to produce

$$\epsilon^2(\omega)-\epsilon(\omega)\left[\frac{1+f\epsilon^0(\omega)}{2}\right](\epsilon_{11}+\epsilon_{10})+f\epsilon^0(\omega)\epsilon_{11}\epsilon_{10}=0\ , \tag{17}$$

where the wave vector K in $\coth(\mathrm{Ka}_1)$ is taken to be the reciprocal of the semimajor axis of the particle in the solution for the long-wavelength mode and the reciprocal of the semiminor axis in the solution for the short-wavelength mode. Equation (17) is used in finding the surface-plasmon resonant values of the dielectric function. These values replace ϵ_{11} and ϵ_{10} in the polarizabilities. A numerical routine was developed for Eq. (17) using stored files of optical data.[10] In Sec. IV we compare the results with the experiments we performed.

IV. RESULTS

Figure 4 shows typical absorption spectra of polarized light for heat-treated silver particles on a transparent sub-

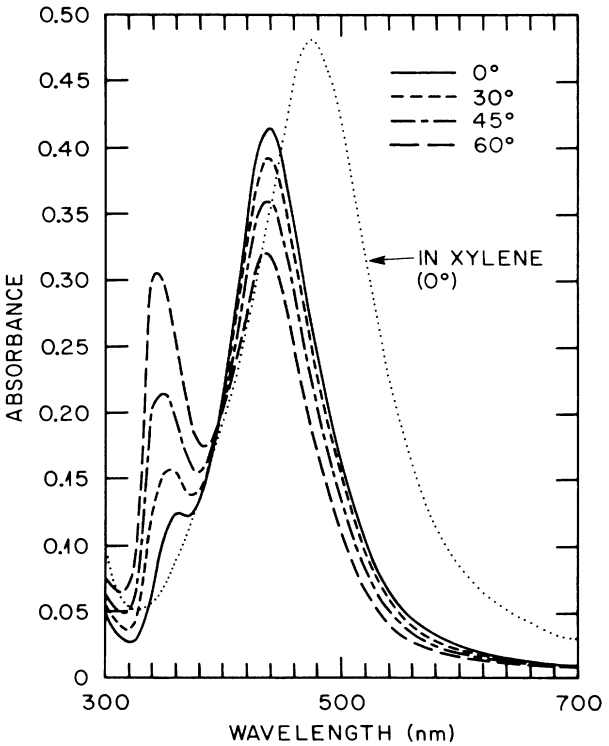

FIG. 4. Experimental absorbance in p-polarized light of a 4-nm silver film on quartz heat treated at 200 °C for 1 min. Angles of illumination are from the normal to the surface. Also, one absorbance at normal incidence with a quartz cover slide using xylene as an index-matching fluid is shown. All measurements were made using a corresponding sample without silver as a reference.

strate. The long-wavelength peak near 440 nm is seen to decrease with angle of incidence in the p-polarized spectra, whereas the corresponding peak in s polarization increases (not shown). The short-wavelength peak near 340 nm appears only weakly when using the s polarization but grows with angle in p-polarized illumination. In s-polarized light the electric vector is always aligned along the major axes of the spheroidal silver particles, and, being uniform across each particulate, it only directly excites the longer-wavelength mode of oscillation. In p-polarized light a component of the electric vector is aligned along the minor axes, growing with increasing angle, and along the major axes, decreasing with increasing angle. Thus the short-wavelength peak is due to the normal mode of oscillation across the minor axes. The appearance of the spectra is typical for metallic films which form spheroidal particles on transparent substrates. By surrounding the particles with an index-matching fluid, the long-wavelength peak is significantly shifted to lower energies. The short-wavelength peak cannot be clearly observed under the index-matching fluid primarily because of the limitation in incidence angle (due to refraction effects) with the present arrangement. The titanium oxide films have a strong absorption in the region of the short-wavelength resonance, preventing observation of that resonance.

Figure 5 shows theoretical curves using model oblate spheroids on a quartz substrate. The absorbance was calculated as

$$A=-\sum_{R=0}^{1}\log_{10}[1-N\sigma f(R)]\ ,$$

where

$$N=N_0 f(R)/\cos\theta$$

and

$$f(R)=(e^{-[(R_0-R)^2/2R_s^2]})\Big/\sum_{R=0}^{1}f(R)\ ,$$

where N_0 gives the number of particles per unit area at normal incidence and N gives the number of particles within the probe beam area as a function of angle θ. (N_0 was not explicitly determined but evaluated from the evaporation thickness which is N_0 times the individual particle volume.) The distribution of particle shapes was arbitrarily assumed to be Gaussian in R given by $f(R)$, centered at R_0 with a width of R_s. These curves were generated using the experimental evaporation thickness of 4 nm and by fitting to the experiment with the parameters of the Gaussian shape profile. The peak positions and shapes agree well with the experimental curves except for a shoulder in the experimental curves near 360 nm. This position of this shoulder suggests the presence of a substantial number of small particles which are more closely spherical in shape rather than oblate. These particles are difficult to resolve in a scanning electron microscope. Additionally, since the long-wavelength peak is too strong theoretically (using the entire volume corresponding to 4-nm evaporation thickness), some of the excess is likely due to the spherically shaped particles. These particles may be resolved in the future using scanning-tunneling microscopy. The Gaussian profile would be replaced with a measured profile of shapes should experimental microscopic data be made available in the future. The angular dependence of the height of the absolute absorbance peaks appears to be only qualitative. The present theory does not include the variation in overlap of cross section between neighboring particles. This factor and multiple reflections in the quartz should be calculated in order to improve the model presented here. The predicted shift in the long-wavelength peak under xylene is given well by the current theory, substantiating the effect of the substrate on the particle resonance positions. The peak positions are the key pieces of information needed to determine the shape.

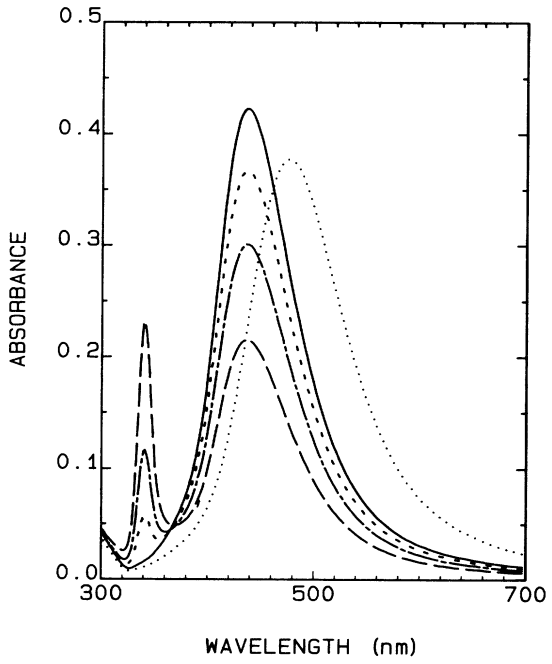

FIG. 5. Theoretical absorbance using the experimental evaporation thickness of 4 nm and a Gaussian distribution of particle shapes of $R_0=0.38$ and $R_s=0.1$. The angles shown are 0°, 30°, 45°, and 60° with the short-wavelength peak growing with increasing angle. Also shown is the absorbance at normal incidence with the same particles surrounded in a uniform silica medium.

Figure 6 shows the theoretical position of the resonance peaks as a function of particle shape for isolated particles, particles on a silica substrate [Eq. (14)], and particles surrounded by a medium with a dielectric response of silica (given by the wavelength at which the dielectric function of silver is $\epsilon_0\epsilon_{10}$ or $\epsilon_0\epsilon_{11}$). The short-wavelength branch (normal mode) shows little shift in wavelength due to the presence of the substrate, and thus the experimental peak is observed relatively unperturbed from the isolated particle resonance. The long-wavelength branch (tangential mode) shows a substantial shift from the isolated particle resonance, about half the total shift in going from isolated particle resonance to the completely surrounded case.

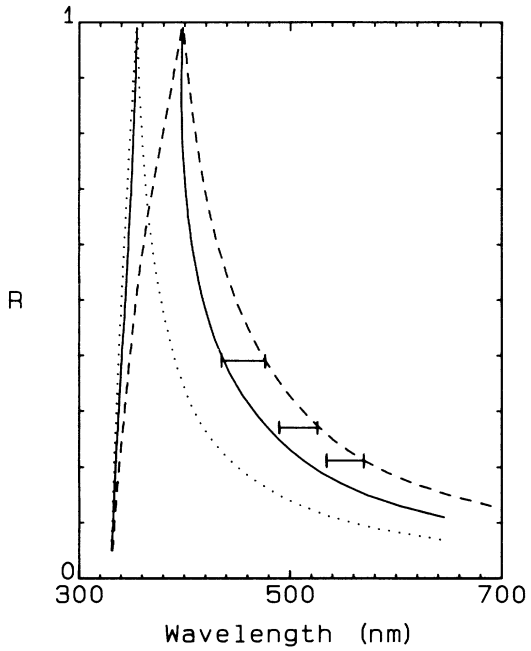

FIG. 6. Calculated position of silver spheroid resonances as a function of minor—to—major-axis ratio (R). Curves extending to short wavelengths describe surface-plasmon oscillations across the minor axis ($l=1$, $m=0$), while the curves extending to long wavelengths describe oscillations across the major axis ($l=1$, $m=1$). Dotted line: particle in vacuum; solid line: particle on quartz; dashed line: particle fully surrounded by a medium with an index of refraction of quartz. Also shown as horizontal bars are the experimental shifts observed when the particles are enclosed by xylene with a quartz cover.

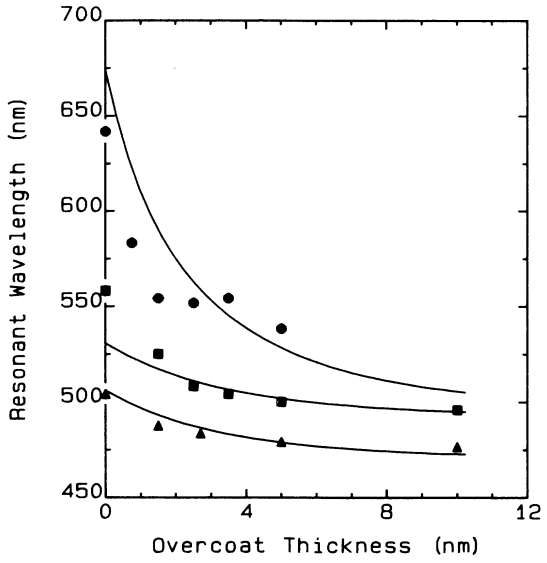

FIG. 7. Position of the long-wavelength ($l=1$, $m=1$) resonance for silver spheroids on silica overcoated substrates as a function of the overcoat thickness. Points: experimental; curves: theory. (1) Titanium oxide substrate, $R=0.32$. (2) Lead fluoride substrate (unheated silver particles), $R=0.34$. (3) Lead fluoride substrate (heat-treated silver particles), $R=0.45$.

This is consistent with the experimental measurement of the shift as silver particles on silica were covered with an index-matching fluid for three particle shapes (horizontal bars in figure). This figure also points out the inapplicability of the theory to particles close to the spherical limit. The long-wavelength peak is obviously too greatly shifted from the isolated particle case at $R=1$, since it appears at the same wavelength as the fully surrounded case. A theoretical model with a less tight coupling with the substrate is needed here.

The effect of proximity of a moderately depolarizing substrate is seen most clearly by varying the distance of the particle film from the substrate using an intermediate evaporated silica layer. The dependence of the resonance position of the long-wavelength peak of silver particles is shown in Fig. 7 as a function of evaporated silica layer thickness. The circles are the experimentally determined resonance positions for independently fabricated samples which were treated identically except for silica thickness. Lead fluoride and titanium dioxide were chosen for their transparency and for their high index of refraction (relative to silica) to show the effect most clearly. The resonance is shifted to lower energies as the particles are brought closer to the surface. The effect is short range (less than about 10 nm) since the surface-plasmon fields from the particles rapidly decay with distance. Also shown is the resonance position calculated from Eq. (17). The shape of each of the three particle types was determined empirically in each case from the best fit with the theory. The wave vector K was calculated from an average major diameter of 20 nm from electron micrographs of similarly prepared samples. The experiment and theory agree well within the limitations of consistent sample preparation.

V. CONCLUSIONS

Annealed metal-island films can form particles which can be modeled as oblate spheroids which can resonate with an external time-varying field. The two dipole modes of oscillation are observed and are affected by the depolarizating interaction with the underlying substrate. The charge oscillation of the particle normal to the surface is affected little by the substrate. In contrast, the mode parallel to the surface is seen to shift considerably to lower energies. These effects were further demonstrated by (1) imbedding the particles in a uniform dielectric medium and (2) varying the distance of the particles from the surface of the substrate. A method for calculating the dielectric response of a spheroid resting on a substrate is given and is shown to be in agreement with experiment.

ACKNOWLEDGMENTS

This work was sponsored by the Department of the Army under Interagency Agreement Nos. DOE 40-1294-82 and ARMY 3311-1450 and the Office of Health and Environmental Research, U. S. Department of Energy, under Contract No. DE-AC05-840R21400 with Martin Marietta Energy Systems, Inc.

[1]K. Estermann, Z. Phys. Chem. **106**, 403 (1923); Z. Phys. **33**, 320 (1925); see also, O. Heavens, *Optical Properties of Thin Solid Films* (Dover, New York, 1965).

[2]J. W. Little, T. L. Ferrell, T. A. Callcott, and E. T. Arakawa, Phys. Rev. B **26**, 5953 (1982).

[3]J. W. Little, T. A. Callcott, T. L. Ferrell, and E. T. Arakawa, Phys. Rev. B **29**, 1606 (1984).

[4]S. W. Kennerly, J. W. Little, R. J. Warmack, and T. L. Ferrell, Phys. Rev. B **29**, 2926 (1984).

[5]R. J. Warmack and S. L. Humphrey, Phys. Rev. B **34**, 2246 (1986).

[6]J. K. Gimzewski, A. Humbert, J. G. Bednorz, and B. Reihl, Phys. Rev. Lett. **55**, 951 (1985).

[7]S. A. Lyon and J. M. Worlock, Phys. Rev. Lett. **51**, 593 (1983).

[8]J. P. Goudonnet, T. Inagaki, T. L. Ferrell, R. J. Warmack, M. C. Buncick, and E. T. Arakawa, Chem. Phys. **106**, 225 (1986).

[9]R. H. Ritchie, J. C. Ashley, and T. L. Ferrell, in *Electromagnetic Surface Modes*, edited by A. B. Boardman (Wiley, New York, 1982), Chap. 3.

[10]H. J. Hageman, W. Gudat, and C. Kunz, Deutsches Electronen-Synchrotron (Hamburg) Report No. Desy-Sr-74/7, 1974 (unpublished).

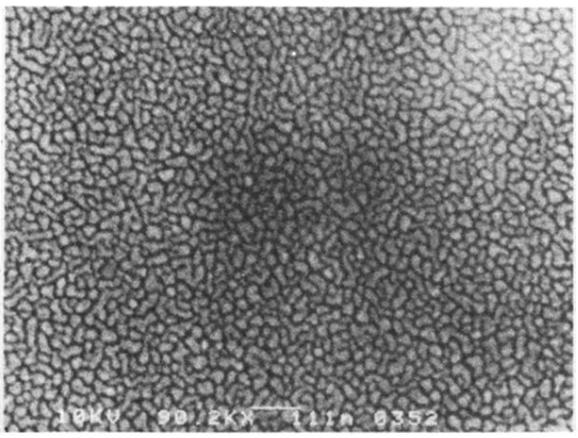

FIG. 1. Scanning electron micrograph of a thin (5-nm) silver evaporation on silicon at room temperature. Bar indicates a length of 111 nm.

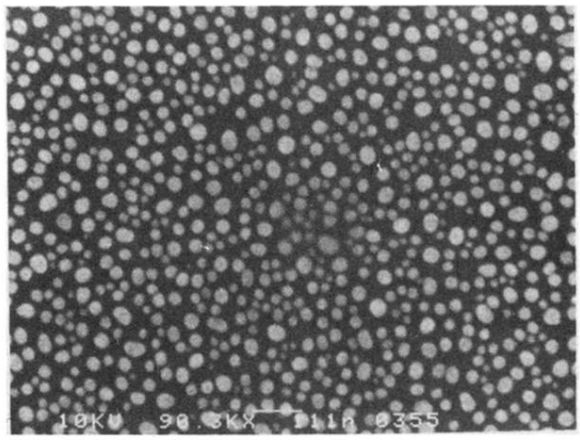

FIG. 2. Evaporated silver film on silicon after a 1-min anneal at 200°C. Same scale as Fig. 1.

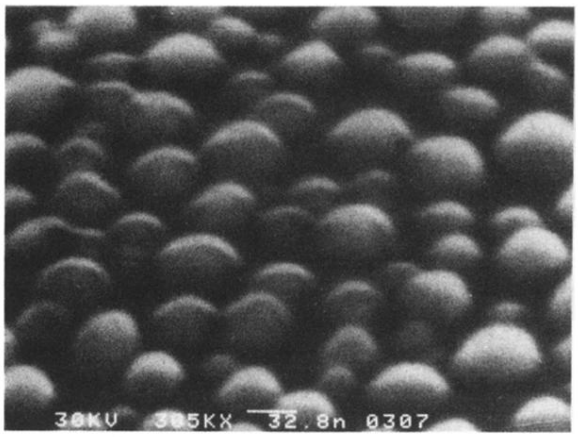

FIG. 3. Evaporated and annealed silver film on silicon viewed at 60° from normal showing the oblate shape of the particles. Bar indicates a length of 32.8 nm.